A piezo-electrically actuated valve for hydraulic exoskeleton drives — modelling and measurement of a prototype

Philipp Albrecht-Zagar*, Rudolf Scheidl

Johannes Kepler University Linz, Institute of Machine Design and Hydraulic Drives, philipp.albrecht-zagar@jku.at

Abstract

This paper deals with the development of a prototype for a piezo-electrically actuated hydraulic spool valve which shall be used as a low-power, miniaturized hydraulic valve for e.g. exoskeleton applications where size, weight and efficiency plays a crucial role. The two main ideas of the hydraulic valve are (i) using a buckling beam as an element which amplifies the displacement of the piezo stack and provides bistable behavior and (ii) introducing a resonant mechanical system consisting of the valve's spool and two springs which is excited by the coupling to the piezo stack. The resulting valve is a bistable, piezo-electrically switched hydraulic 4/2-valve. The paper first explains the valve concept and the design of the valve prototype. A mathematical model for the piezoelectric actuator is derived by using higher order beam theory. A Ritz-Ansatz is introduced to get approximate expressions for the beam displacement and which proves to predict measurements very well. In a next step, the model is extended to describe the complete system. This system consists of a lumped, quasi-static piezo stack model which is coupled to the approximated beam solution, equations of motion of the spool and hydraulics. Numerical simulations prove the working principle of the valve and give insights of how parameters such as the spring stiffness affect the switching time and the pressure built-up at the output of the valve.

River Journal, 1–19.

Keywords: piezo electric actuator, hydraulic valve design, bistable, mathematic modelling.

1 Introduction

Modern applications of hydraulics such as exoskeleton drives for medical or military use demand for small and light-weight hydraulic valves [1]. Typically, valves for such applications are switched electromagnetically which is not only bulky but also costly and inefficient in terms of energy demand. The last point is especially relevant for battery-driven applications. To overcome these disadvantages of magnetically actuated valves the use of piezoelectric [3] or magnetostrictive [2] materials can increase the power density and pave the way to miniaturized hydraulic components. Besides these advantages, using smart materials for valve actuation also introduces some downsides. Simic et al. highlighted the advantages and disadvantages of the use of piezo-electric materials for valve actuation [4].
Within the last two decades several different approaches for valves using piezo-electric actuators where investigated. Especially, a lot of research was done on the actuation of servo valves with different types of actuator designs such as piezo stack actuators, bimorph benders, ring benders and amplified piezo stacks. A detailed review for such piezo-actuated servo-valves can be seen in e.g. Tamburrano et al. [5]. Other papers deal with the performance evaluation and control of direct actuated servo valves using piezos [6–8]. In the dissertation of Reichert the complete developement of two piezo-actuated servo-valves was systematically investigated [9]. The mentioned papers mainly focus on servo valves which are directly actuated via a piezo actuator. However, in this paper a piezo switching valve is analyzed which uses an amplification mechanism based on a buckled beam as introduced in [10]. Meanwhile, several works on valve switching using such a buckling mechanism where published in the field of hydraulics, such as [11–13]. A prototype for an 4/2-valve is introduced with the aim to analyze two concepts using a piezo-electrically actuated buckling beam as a switching element. Fig. 1 shows a schematic of the prototype. The piezo actuator consists of the piezo stack which is mounted on a spring element. At the end of the spring element a buckling beam is attached which is connected to the spool of a hydraulic 4/2-valve. Two springs on the left and right hand side of the spool together with the spool mass

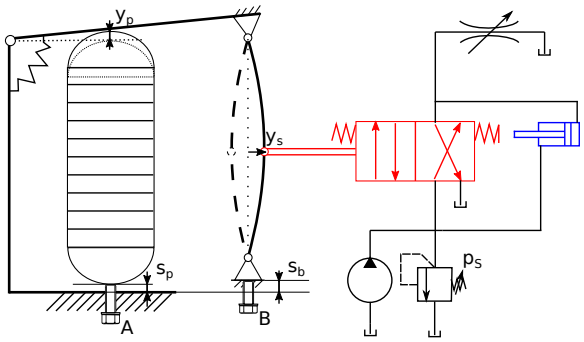

Figure 1 Schematic of a hydraulic valve prototype.

create a mass-spring system which is held in either the left or right position depending on the buckled beam's stationary point. When the beam swings from one end-position to the other by actuating the piezo stack the valve is switched. Fig. 2 shows the two concepts (*a* and *b*):

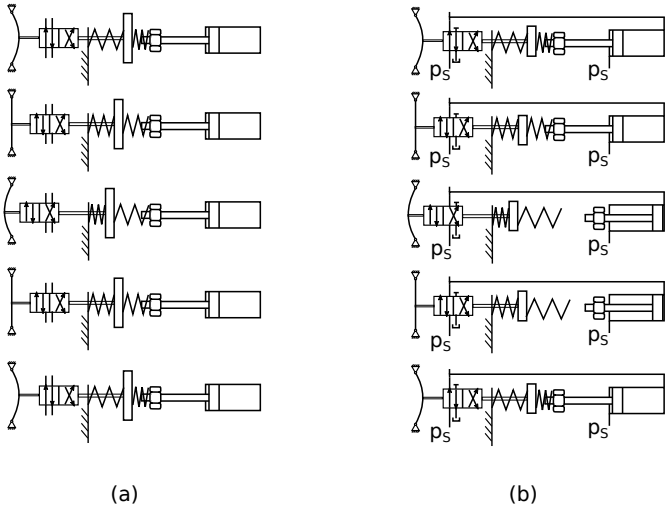

Figure 2 Schematic of a different switching phases of hydraulic valve prototype for concept *a* and *b*.

Direct actuation of spool In this concept in order to switch the valve the piezo actuator directly affects the spool's position. If the beam initially is buckled towards the right and the spool shall be moved from

right to left, the piezo actuator opens the spring element to straighten the beam. This accelerates the spool until it reaches a dead point where the beam is straight and no lateral force can be applied through the actuator anymore. Due to the spool's inertia this dead zone is passed and the piezo actuator starts closing the spring element again which leads to a buckling of the beam in the direction of movement. The spool ends up at a position which corresponds to the left buckled beam's stationary point when the piezo stack is closed.
This concept demands for a large piezo actuator. By assuming the spool displacement to be in the range of one mm and that a displacement amplification mechanism amplifies the piezo stack displacement by a factor of 50, the piezo stack must have a nominal travel range of $20\mu m$ and therefore a stack length of $\approx 20mm$. The fact that the moving parts (spool and manipulator of actuator) have to travel through the dead zone without actuation only due to inertia, low friction is necessary in the bearings of the beam as well as in the sealing gaps of the valve. In particular this becomes crucial for miniaturized valves such as needed for exoskeleton applications where masses should be very low. In contrast to magnetically switched valves the actuation happens electrostatically by loading the piezo's capacitance, so only the resistive and hysteretic losses during the switching process are degrading efficiency.

Hydraulic feedback actuation and snap-through mechanism
In this concept the buckled beam has the function of a piezo-electrically adjustable snap-through element. When the spool position is on the right hand side a small hydraulic cylinder is fed by the valve's output which applies a force via a spring on the spool in the direction that would drive the spool to the left position. This force is compensated by the buckled beam as long as it is smaller than the minimum needed lateral force for snap-through. For switching the valve, the piezo stack is expanded for a short period of time which slightly straightens the buckled beam. This decreases the needed lateral force for snap-through and the valve switches. Doing so, the beam buckles to the left, thereby, compressing the spring on the left which acts on the spool. The valve's output is fed back to the hydraulic cylinder which moves the cylinder to the right. At this state the force of the left spring and the lateral force of the buckling beam are compensating each other and the spool is at rest on the left hand side. Switching back also happens by

expanding the piezo stack for a short period of time. The force on the spool which is applied from the left spring then exceeds the lateral force for snap-through and the spool swings to the right position. This lets the hydraulic cylinder move to the left which applies a force on the right spring of the spool. A critical design parameter is the delay with which the hydraulic cylinder feeds back the output signal.

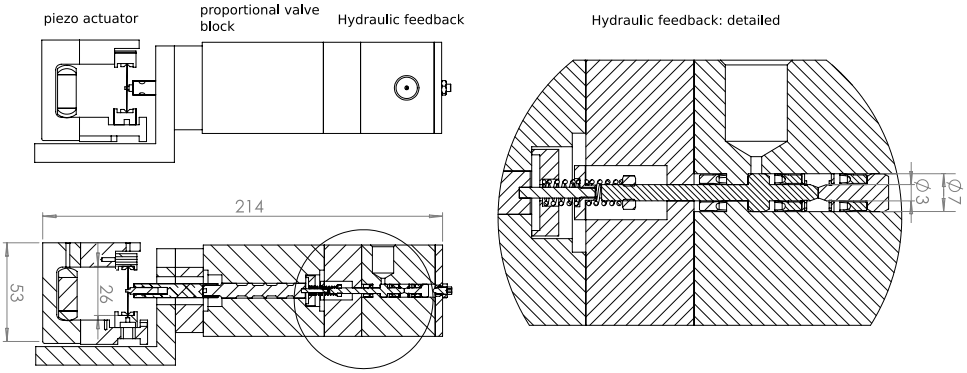

Figure 3 Technical drawing of valve prototype.

Fig. 3 shows the design of both, the piezo actuator and the hydraulic module which includes two springs attached at the valve's spool as well as the small hydraulic cylinder which establishes a feedback loop to the spool. For the prototype the valve block and the spool of a closed loop proportional valve (NG6 from Bosch Rexroth) was used as such valves exhibit zero overlap which is preferred in this applications with low spool displacement. The spool is connected to the buckling beam via a rivet on the left hand side and to a spring suspension consisting of two springs via a $M2$ screw thread on the right hand side. This allows the spool to be axially adjusted to the zero position of the valve when the beam is not buckled by rotation around its axis. The spring suspension's left side sits on the proportional valve block. The right side can be either free or in contact with the hydraulic feedback element depending on the switching state of the valve and hence the fed back pressure in the hydraulic feedback cylinder.

2 Modeling

2.1 Buckling Beam

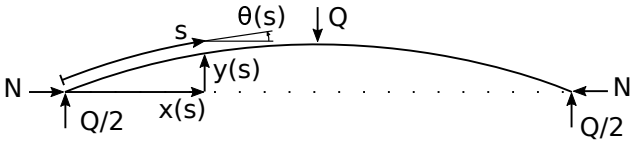

Figure 4 Schematic of the valve prototype.

Fig. 4 shows the free body diagram of a pin ended buckling beam with a normal force N at the end joints and a transversal force Q applied in the middle of the beam. s is the coordinate along the beam and $x(s)$ and $y(s)$ is the horizontal and transversal displacement of the point at s respectively. Due to symmetry only one half of the beam must be considered and the governing equation of the static buckling beam becomes

$$yN - xQ/2 = EI\frac{\mathrm{d}\theta}{\mathrm{d}s} \qquad \forall s \in (0, L/2) \tag{1}$$

where E is the elastic modulus of the beam's material, I is the area moment of inertia and $\theta(s)$ is the tangent angle at position s on the beam. The right hand side of equation (1) describes the bending moment in the beam which is proportional to the beam's curvature $\mathrm{d}\theta/\,\mathrm{d}s$. By using the relation $\mathrm{d}y = \mathrm{d}s\sin(\theta)$ this expression expands to $\mathrm{d}\theta/\,\mathrm{d}s = \mathrm{d}^2y/\,\mathrm{d}s^2/\sqrt{1-(\mathrm{d}y/\,\mathrm{d}s)^2}$. Inserting this expression and $x(s) = \int\sqrt{1-(\mathrm{d}y/\,\mathrm{d}s)^2}$ into (1) with subsequent approximation to the fourth order terms of $\mathrm{d}y/\,\mathrm{d}s$ this leads to the equation

$$D(y, y', y'') = -\frac{yN}{EI} + \frac{Q\int_0^s 1 - {y'}^2/2\,\mathrm{d}s}{2EI} - y''\left(1 + {y'}^2/2\right) = 0. \tag{2}$$

Using the ansatz function $\hat{y}(s) = A\sin(\omega s)$ and inserting it into the differential operator $D(y, y', y'')$ in (2) results in a non-zero residual. To calculate the parameter A via the method of Galerkin, the ansatz function itself is utilized as a weighting function. This results in the orthogonality condition

$$\left\langle D(\hat{y}, \hat{y}', \hat{y}''), \hat{y}\right\rangle = 0. \tag{3}$$

Inserting the relations

$$q = Q/N_{cr}, \quad n = N/N_{cr}, \quad a = A/L$$

with the beam length L and the critical buckling load $N_{cr} = EI\omega^2$ equation (3) solves to

$$n = \frac{3\pi^4 a^3 - 16\pi^2 a^2 q + 24\pi^2 a + 48q}{24\pi^2 a}. \tag{4}$$

The variable a is the beam's deflection related to the beam length L which is the same as the related spool displacement when the beam is connected as shown in Fig. 3. Hence, Eq. (4) approximates the relation between the applied vertical and lateral forces and the elastic deformation of the beam considering the first buckling mode. The distance between both clamped points is

$$\Delta L = 2\int_0^{L/2} \sqrt{1 - y'} ds - L = \frac{a^2\pi^2}{4}. \tag{5}$$

2.2 Piezo stack actuator

In the next step a static model for the piezo actuator is derived. Starting point is the IEEE standard model [14] for piezoelectric materials Std 176-1987 with its governing equations

$$D = \varepsilon E + c_P \sigma \tag{6a}$$

$$S = c_P E + c_E \sigma \tag{6b}$$

with the electric flux density field D, the electric field E, the strain tensor of the piezo material S and the mechanical stress tensor σ. The tensor c_P is the piezoelectric coefficient, c_E the elastic compliance and ε the permittivity of the piezo electric material. Eqs. (6) describe the predominant conditions at an arbitrary point in the piezo material. This can be simplified to get lumped system parameters by considering only uniaxial field quantities. Using basic piezo stack parameters such as the area A, the number for piezo slices for the stack N and the height of

one slice h the fields in (6) can be written as

$$D = \frac{Q}{NA} \qquad E = \frac{U_p}{h} \tag{7a}$$

$$\sigma = \frac{F_p}{A} \qquad S = \frac{Y_p}{Nh} - 1. \tag{7b}$$

Inserting in (6) results in a displacement $Y_p(U_p, F_p)$ can be written as

$$Y_p = U_p k_p - k_e F_p \tag{8}$$

with the piezo voltage U_p, the piezo force F_p and two constants k_e and k_p which consider the piezo effect and the mechanical stiffness of the piezo material respectively.

Momentum balance for the upper part of the U-form in the static case

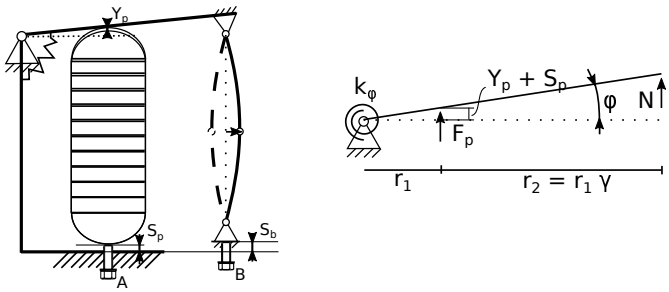

Figure 5 Schematic of the piezo actuator and the free body diagram of the piezo actuator's upper part.

(see Fig. 5) results for small angles $\varphi \approx (Y_p + S_p)/r_1$ in

$$F_p + N\gamma = C_u(Y_p + S_p) \tag{9}$$

with the transmission ratio $\gamma = r_1/r_2$ and the equivalent linear spring constant at the piezo position $C_u = k_\varphi/r_1^2$. The length S_p is adjusted through screw A (Fig. 5) and is needed to preload the piezo stack. To adjust the buckled equilibrium position of the beam screw B (Fig. 5) is used. The displacement via screw B basically acts on two serially connected spring systems: the buckled beam in normal direction and the U-form spring element. Hence, the displacement of the upper clamping position of the buckling beam $S_b - \gamma(Y_p(U_p) - Y_p(0))$ is the sum of the change of the buckling beam's vertical length ΔL (Eq. (5))

and the displacement of the U-form spring element:

$$S_b - \gamma(Y_p(U_p) - Y_p(0)) = \frac{a^2\pi^2}{4} + \gamma^2 N/C_u. \tag{10}$$

Inserting (8) in (9), solving for the piezo displacement $Y_p(U_p)$ and converting the result into non-dimensionless form by relating every length to the beam length L and substituting $u = U_p/U_{max}$ expression (10) becomes

$$s_b - u\frac{\gamma\kappa_p}{c_U\kappa_e + 1} = \frac{\gamma^2 n}{c_U} + \frac{a^2\pi^2}{4}. \tag{11}$$

This equation together with Eq. (4) describes the static model behavior of the piezo actuator. It relates the non-dimensional voltage u, the non-dimensional lateral force q and the non-dimensional lateral buckling displacement a in an algebraic expression which is evaluated by measurements in the next section.

2.3 Spool valve and hydraulics

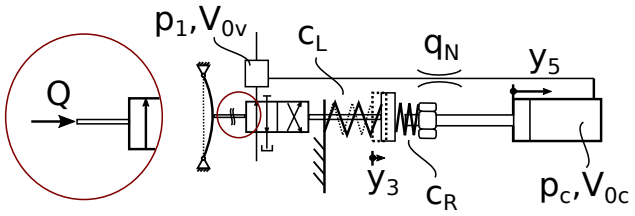

Figure 6 Technical sketch for spool and hydraulics modeling.

The state space representation of the system which is sketched in Fig. 6 considers six states, i.e. the pressures p_1 and p_c at the output of the valve and the chamber of the feedback cylinder as well as displacement and velocity for the spool mass (y_3,$\dot{y_3}$) and the feedback cylinder (y_5,$\dot{y_5}$).
First, the equation of motion for the spool is derived: Fig. 6 shows the spool element which is connected to the buckling beam on the left side and which is fixed between two spring elements with constants c_L and c_R. When the feedback cylinder is at position $y_5 = 0$ the spring elements are preloaded since the screw nut on the cylinder rod presses the right spring element to the left. The reaction force from the spring to the cylinder depends on the current position of the spool (or

the buckling beam). Since compression springs which can only act in positive direction, forces from the left and right spring element are

$$F_L = -c_L(y_3 - y_{3,0}),\ F_R = -c_R(y_3 - y_5 + y_{5,0})$$

as long as these values are greater than zero and zeros otherwise. y_3 describes the position of the spool which is the same as the buckling amplitude A (see previous section). Besides F_R and F_L, the lateral force of the buckling beam Q as well as a viscous damping force F_d is acting on the spool. The lateral force Q is as a function of piezo voltage U and displacement y_3.
Together with the equation of motion for the cylinder and the pressure build-up equations for p_1 and p_c the state space model reads as

$$\dot{p_1} = \frac{E}{V_{0,v}} \left(q_L + \frac{y_3}{\hat{y}_3} \frac{q_{N,v}}{\sqrt{p_N}} \sqrt{p_S - p_1} \right) \tag{12a}$$

$$\dot{y_3} = v_3 \tag{12b}$$

$$\dot{v_3} = \frac{1}{m_s}(F_L + F_R + Q(y_3, U) - d_f v_3) \tag{12c}$$

$$\dot{p_c} = \frac{E}{V_{0,c} - A_A(y_5 - s_c)} \left(v_5 A_A + \frac{q_{N,t}}{\sqrt{p_N}} \sqrt{p_1 - p_c} \right) \tag{12d}$$

$$\dot{y_5} = v_5 \tag{12e}$$

$$\dot{v_5} = \frac{1}{m_c}(-p_c A_A + p_S A_B - F_R + F_c) \tag{12f}$$

where q_L is the load at the output of the valve, m_s is the spool mass, m_c is the cylinder mass, $q_{N,v}$ and $q_{N,t}$ are the nominal flow rate of the valve when opened with $\hat{y}_3$ and the nominal flow of the throttle in the feedback loop, respectively, d_f is a factor which includes dissipation through velocity proportional friction. Eqs. (12) considers the feedback cylinder and hence models valve concept b which was explained in section 1. For simulation of the concept a this model reduces to

$$\dot{p_1} = \frac{E}{V_{0,v}} \left(q_L + \frac{y_3}{\hat{y}_3} \frac{q_{N,v}}{\sqrt{p_N}} \sqrt{p_S - p_1} \right) \tag{13a}$$

$$\dot{y_3} = v_3 \tag{13b}$$

$$\dot{v_3} = \frac{1}{m_s}(F_L + F_R + Q(y_3, U) - d_f v_3) \tag{13c}$$

and the force $F_R = F_R(y_3, y_5)$ evaluated at $y_5 = 0$.

3 Measurements and Simulations

Table 1 Values for simulation model of valve prototype

valve and hydraulics			
p_S	100 bar	p_T	1 bar
E	14000 bar	V_{0v}	1.0 l
V_{0c}	2.0 l	q_{Nv}	40 l/min
$q_N t$	8 l/min	A_A	38.5 mm^2
A_B	31.4 mm^2	$\hat{y}_5$	0.3 mm
m_s	5 g	c_L, c_R	16 N/mm
piezo actuator			
κ_e	5.7×10^{-6}	κ_p	3.7×10^{-4}
c_U	9.7×10^{-3}	γ	4.5
beam			
B	10 mm	H	0.3 mm
E_{steel}	180 kN/mm^2	l_0	26.9 mm
s_b	270 µm		

3.1 Piezo actuator

The model for the piezo stack actuator was verified through measurements of lateral displacement of the buckling beam, normal force N at the clamping points of the beam and lateral force Q. Fig. 7 shows some results for those quantities for a piezo actuator with a linear spring constant of $C_U = 2N/m$ that was discussed in [15]. In the upper diagram on the left the lateral displacement as a function of the normal force N is shown. Theory suggests that the beam remains straight until the buckling force N_{cr} is reached. At this bifurcation the beam can buckle towards both sides. Due to imperfections of the beam measurements (red, blue) show that the beam already starts buckling at lower normal forces, that it buckles always on a preferred side and that theory represents the asymptotic behavior to which the measurement converges for high and low normal forces. Also, severe hysteresis can be seen which is due to friction in the beam's joints. In the upper diagram of the right hand side graphs show the lateral force Q as a function of beam displacement for theoretical piezo actuators with different linear spring constants c_U. A measurement for an actuator with $c_U = 2$ N/µm proofs the theory to fit well. On the left hand side

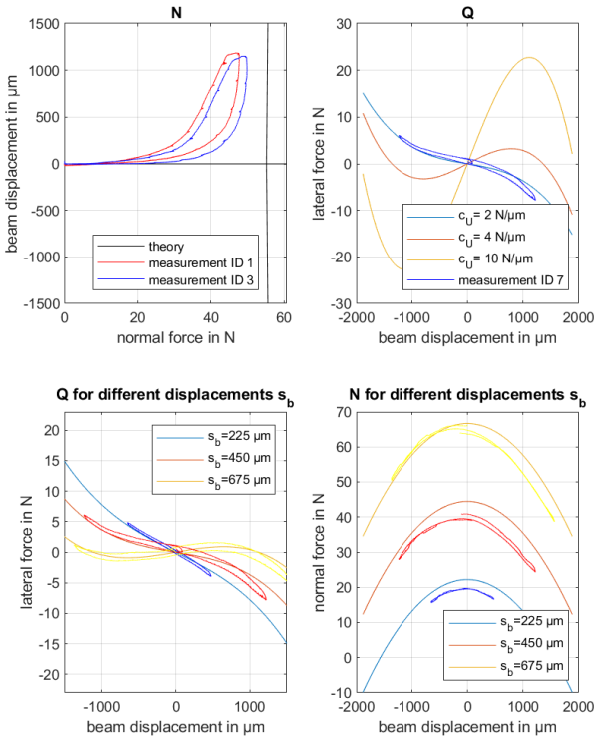

Figure 7 Measurements of a piezo actuator with linear spring constant of $C_U = 2N/m$.

on the bottom graphs show theoretical and real relationships between the lateral force and the beam displacement for an actuator with $c_U = 2$ N/µm and different values for the displacement of the beam screw s_b. For the same values of s_b the bottom right diagram shows theory and measurements of the normal force N as function of beam displacement. These measurements proof that the theory derived in section 2 works very well and is suitable for prototype design as well as for simulation of the prototype valve. One disadvantage when using piezo materials is the severe hysteresis (see [4,5]). Such effects can be modelled by using e.g. a Preisach-model [17], however, the reader should be aware of, that

within this paper such type of nonlinearity was not consindered in the simulation.

3.2 Piezo valve

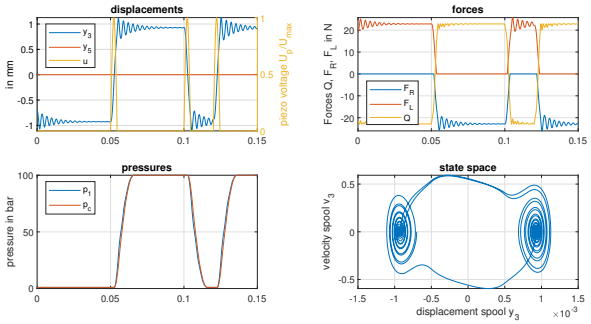

Figure 8 Simulation of valve concept *a*: optimal switching behavior

Valve concept *a* Fig. 8 shows a simulation of the valve concept *a*. The upper left diagram shows that the switching time of the valve in both directions is approximately $t_s = t_{10\%} - t_{90\%} \approx 3.1$ ms and the same due to symmetry for both directions. After reaching the opened or closed state the spool oscillates with a frequency of $f \approx 303$ Hz which corresponds to the approximate beams natural frequency of

$$f_0 = \frac{1}{2\pi}\sqrt{c/m} = 310\text{Hz}$$

with $c = EI\pi^4/(2L^3)$ and $m = m_s + \rho BHL/2$ which is derived by a Ritz-Ansatz in [16]. In the upper right diagram the interplay of the spring forces F_L and F_R as well as the lateral force Q applied from the beam is shown. On the bottom right hand side the phase space representation of the spool's motion is shown. One can see the two attracting local minima which exist if the nondimensional piezo voltage u is low enough. This concept demands for a piezo actuator which can fully open such that the beam can swing from one side to the other almost freely without the need to snap-through. Therefore, the disadvantage to concept *b* is the need for a big piezo stack which makes the actuator less useful for miniaturization and expensive. The graphs in Fig. 9 on the top show how different nondimensional switching

voltages ($u_1 = 1.0$, $u_2 = 0.6$, $u_3 = 0.8$) affect the swichting behavior. For a small value of $u_2 = 0.8$ the switching process is not successful. The two diagrams on the bottom show an approximated behavior of the valve with an imperfect beam which is plastically deformed in the lateral direction by $\Delta a = 50$ µm. Fig. 9 shows that an actuator with such a beam is not able to switch the valve anymore, even though the spool displacement is already getting positive for some time.

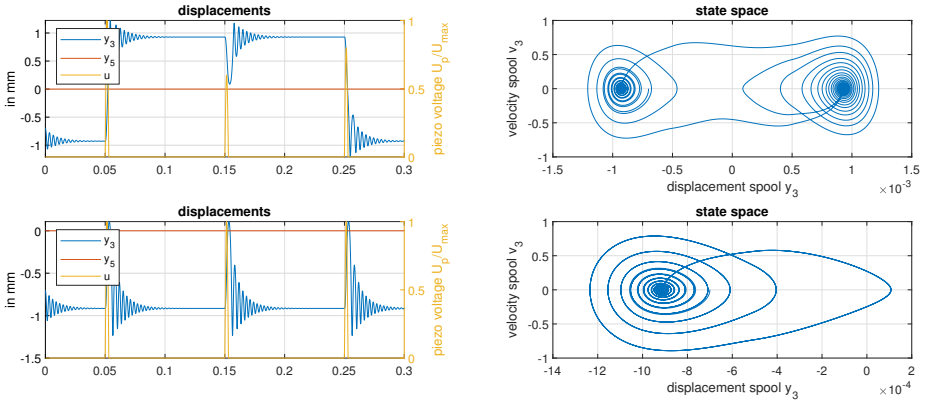

Figure 9 Simulation of valve concept a: switching errors due to small voltages and beam imperfections

valve concept b Fig. 10 shows the simulation results for the valve concept b which uses hydraulic feedback to ease the switching process. This relaxes the demand for big piezo stacks as needed in concept a. The top left diagram shows three successful switching processes. Notice that a nondimensional voltage of $u = 0.6$ is applied which already led to malfunction of concept a. In Fig. 10 one can realize an unequal behavior for different switching directions which is caused by an asymmetric design: If no buckling beam was there, the spool together with the two spring elements act as a mass-spring system. The equilibrium point is defined by the preload of the springs. The function of the feedback cylinder is to switch between two preload forces, hence, change the equilibrium point towards the right or left. The rod side chamber of the cylinder is always pressurized with system pressure. At the other side the output pressure, which is either $p_A = p_S$ or $p_A = 0$ bar, is

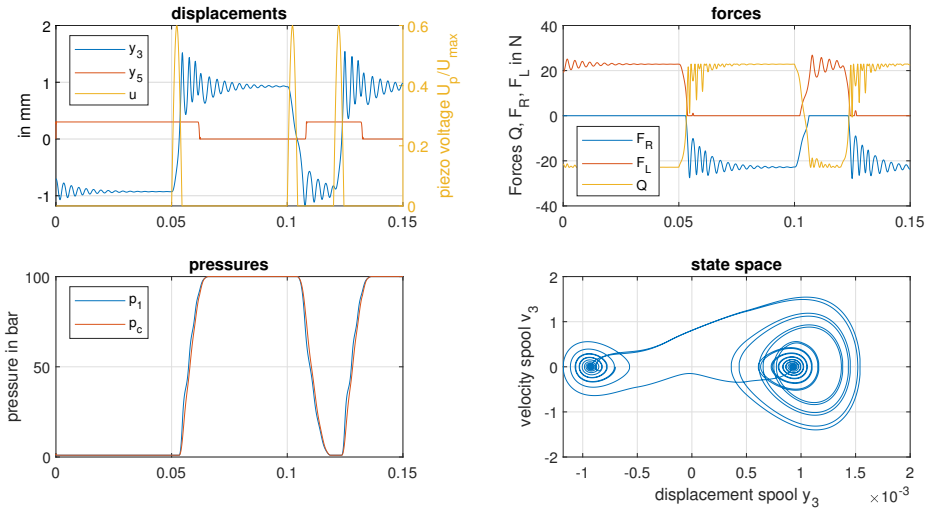

Figure 10 Simulation of valve concept *b*.

applied which makes the cylinder starts moving at

$$p_c = p_S A_B / A_A.$$

For parameters listed in table 1 $p_c \approx 81$ bar. This asymmetric (not at $(p_{v,max} - p_{v,min})/2 = 50$ bar) switching condition is the reason for the seen switching behavior. For the first and third switching process (at $t_1 = 0.05$ s and $t_3 = 0.12$ s) the spool shoots. During this phase the hydraulic cylinder position is still $y_5 = 0.3$ mm, the output pressure is fed back towards the piston and the pressure p_c grows. When the pressure hits $p_c \approx 81$ bar the piston moves in the negative direction, hits against the spring system and applies a higher preload to it. This makes the equilibrium point of the spool move towards the negative direction where the spool finally settles. In the phase space portrait on the bottom right in Fig. 10 this can be seen by two overlaying spirals on the right which converge to two different equilibrium positions. When switching of the spool from $y_3 > 0$ to $y_3 < 0$ which can be seen at $t_1 = 0.1$ s the shift of the equilibrium position happens earlier and during the switching process because the condition $p_c < 81$ bar is met very fast.

4 Conclusion

Two concepts for a piezo-actuated valve are presented in this paper. First a static model of the piezo actuator is presented and verified by measurements. Using the derived models simulations show that concept *a* exhibits symmetric switching behavior but is more sensitive to e.g. imperfections of the buckling beam. Concept *a* also demands for an actuator which exhibits high displacements. This can be seen, as the switching process fails when lower voltage is applied. This necessity raises the costs of the piezo stack and makes the concept unsuitable for miniaturization. Concept *b* overcomes these problems by using an additional hydraulic feedback cylinder which results in successful switching for low voltages which is not possible with concept *a*.

Acknowledgment

This work has been supported by the COMET-K2 Center of the Linz Center of Mechatronics (LCM) funded by the Austrian federal government and the federal state of Upper Austria.

References

[1] R. Scheidl, Digital fluid power for exoskeleton actuation - guidelines, opportunities, challenges ,The Ninth Workshop on Digital Fluid Power, September 7-8, 2017, Aalborg, Denmark.

[2] V. Apicella C. S. Clemente, D. Davino, D. Leone and C. Visone, Review of Modeling and Control of Magnetostrictive Actuators, Actuators 2019, 8(2), 45

[3] S. Yokota, K. Akutu, A Fast-Acting Electro-Hydraulic Digital Transducer (A Poppet-Type On-Off Valve using a Multilayered Piezoelectric Device, JSME International Journal, Series II, Vol. 34, No. 4, 1991.

[4] Simic, M.; Herakovic, N. Piezo actuators for the use in hydraulic and pneumatic valves. In Proceedings of the International Conference Fluid Power 2017, Maribor, Slovenia, 14–15 September 2017; University of Maribor Press: Maribor, Slovenia, 2017

[5] Tamburrano P, Sciatti F, Plummer AR, Distaso E, De Palma P, Amirante R. A Review of Novel Architectures of Servovalves Driven by Piezoelectric Actuators. Energies. 2021; 14(16):4858. .

[6] Lindler, J. E., & Anderson, E. H. (2002). Piezoelectric direct drive servovalve. In Smart Structures and Materials 2002: Industrial and Commercial Applications of Smart Structures Technologies (Vol. 4698, pp. 488-496). International Society for Optics and Photonics.

[7] Jeon, J.; Nguyen, Q.H.; Han, Y.M.; Choi, S.B. Design and evaluation of a direct drive valve actuated by piezostack actuator. Adv. Mech. Eng. 2013, 5, 986812.
[8] Han, C.; Hwang, Y.H.; Choi, S.B. Tracking control of a spool displacement in a direct piezoactuator-driven servo valve system. Front. Mater. 2017, 4, 9.
[9] Reichert, M., & Murrenhoff, H. (2010). Development of high-response piezo servovalves for improved performance of electrohydraulic cylinder drives. PhD thesis. Aachen university
[10] Garstenauer, M. (2001). Theoretical and experimental investigations of a novel concept for hydraulic, high-speed, switching valves. PhD thesis. Johannes Kepler University Linz
[11] Scheidl, R., Scherrer, M. & Zagar, P. The buckling beam as actuator element for on-off hydraulic micro valves. International Journal of Hydromechatronics, Vol. 4, No. 1, pp 55-68, 2021.
[12] Scherrer, M., Scheidl, R., & Manhartsgruber, B. Optimization of a Snap Through Spring for a Hydraulic Valve With Hysteresis Response Behavior. Proceedings of the ASME/BATH 2019 Symposium on Fluid Power and Motion Control. ASME/BATH 2019 Symposium on Fluid Power and Motion Control. Longboat Key, Florida, USA. October 7–9, 2019. V001T01A038. ASME.
[13] Scheidl, R, & Mittlböck, S. A Hydraulic Piloting Concept of a Digital Cylinder Drive for Exoskeletons. Proceedings of the BATH/ASME 2018 Symposium on Fluid Power and Motion Control. BATH/ASME 2018 Symposium on Fluid Power and Motion Control. Bath, UK. September 12–14, 2018. V001T01A040. ASME.
[14] An American National Standard — IEEE Standard on Piezoelectricity, ANSI/IEEE Std 176-1987.
[15] Zagar P., Scheidl R., "A piezo-electric valve actuator for hydraulic exoskeleton drives Part I: design": Proceedings of the 2020 IEEE Global Fluid Power Society PhD Symposium (GFPS), October 19-21, 2020, Guilin, CHINA, 2020.
[16] F. Ziegler, "Mechanics of Solids and fluids." Springer-Verlag, New York, Vienna, 1991.
[17] F. Preisach: Über die magnetische Nachwirkung. In: Zeitschrift für Physik. Band 94, 1935, S. 277–302.

Biography

Philipp Albrecht-Zagar. Born May 29th 1989 in Graz (Austria). MSc of Electrical Engineering at Vienna University of Technology in 2014. Industrial research and development experience in Electronics (E+E Elektronik, 2014-2018). Since Sept. 2018 employed at the Johannes Kepler University Linz as junior researcher, university assistant and PhD candidate.

Rudolf Scheidl. Born November 11th 1953 in Scheibbs (Austria). MSc of Mechanical Engineering and Doctorate of Engineering Sciences at Vienna University of Technology. Industrial research and development experience in agricultural machinery (Epple Buxbaum Werke), continuous casting technology (Voest Alpine

Industrieanlagenbau) , and paper mills (Voith). Since Dec. 1990 Full Professor for Mechanical Engineering at the Johannes Kepler University Linz. Research topics: hydraulic drive technology with emphasis on digital fluid power and mechatronic design.